Key Engineering Materials
ISSN: 1662-9795, Vol. 947, pp 77-82
doi:10.4028/p-959z1t

Submitted: 2022-09-02
Revised: 2022-11-21
Accepted: 2022-11-25
Online: 2023-05-31

Towards SiC-Based VUV Pin-Photodiodes - Investigations on 4H-SiC Photodiodes with Shallow Implanted Al Emitters

Michael Schraml[1,2,a*], Niklas Papathanasiou[3,b], Alexander May[2,c], Tilman Weiss[3,d] and Tobias Erlbacher[1,2,e]

[1]Chair of Electron Devices, University of Erlangen-Nuremberg, Cauerstrasse 6, 91058 Erlangen, Germany

[2]Fraunhofer IISB, Schottkystrasse 10, 91058 Erlangen, Germany

[3]sglux GmbH, Richard-Willstätter-Str. 8, 12489 Berlin, Germany

[a]michael.schraml@iisb.fraunhofer.de, [b]papathanasiou@sglux.de, [c]alexander.may@iisb.fraunhofer.de, [d]weiss@sglux.de, [e]tobias.erlbacher@iisb.fraunhofer.de,

Keywords: photodiode, UV, VUV, pin-diode, shallow ion implantation, shallow emitter, spectral responsivity

Abstract. 4H silicon carbide (SiC) based pin photodiodes with a sensitivity in the vacuum ultraviolet spectrum (VUV) demand newly developed emitter doping profiles. This work features the first ever reported 4H-SiC pin photodiodes with an implanted p-emitter and a noticeable sensitivity at a wavelength of 200 nm. As a first step, Aluminum doping profiles produced by low energy ion implantation in 4H-SiC were characterized by secondary-ion mass spectrometry (SIMS). Photodiodes using these shallow emitters are compared to one with a deep p-emitter doping profile employing I-V characteristics and the spectral response. SIMS results demonstrate the possibility of shallow Al-implantation profiles using low implantation energies with all emitter profiles featuring characteristic I-V results. For some shallow doping profiles, a meassurable signal at the upper limit of the VUV spectrum could be demonstrated, paving the way towards 4H-SiC pin photodiodes with sensitivities for wavelengths below 200 nm.

Introduction

A high sensitivity detection of light in the VUV spectrum, ranging between 10 and 200 nm [1], is significant for e.g., space science, semiconductor high-resolution lithography [1] and monitoring of 172 nm excimer radiation curing [2]. Due to its wide bandgap of 3.26 eV [3], which corresponds to a cut-off wavelength of 380 nm, 4H-SiC offers optimal conditions for visible blind UV photodiodes making it the material of choice for UV sensors. Hence, light with longer wavelengths, i.e., light from the visible spectrum, is barely absorbed, and does not impede the measurement of UV light. Owing to the low intrinsic carrier concentration, SiC also shows an extremely low reverse dark current even at elevated temperatures [3]. This property makes SiC based photodiodes advantageous for low signal detection. In combination with its high thermal conductivity up to 4.9 W cm^{-1} K^{-1} [3] and high chemical stability [3], SiC based photodiodes are exceedingly suitable for operation under harsh environments.

State of the art SiC UV Schottky photodiodes are already capable of detecting VUV light [4, 5]. However, no VUV sensitive 4H-SiC pin-type photodiode has been reported in literature. A higher sensitivity can be expected for pin-photodiodes since the usage of a front metal, which otherwise strongly absorbs UV light particularly at short wavelengths [6], is avoided. Two different methods of p-emitter fabrication have been reported in literature, namely epitaxy of a p-doped layer with subsequent mesa etching [7, 8] as well as ion-implantation [7, 9].

In this work, ion-implantation will be employed since the utilized planar technology avoids the extensive mesa etching and allows fabrication of a shallower p-emitter. This is essential for achieving sensitivities below wavelengths of 200 nm as shorter wavelengths are strongly absorbed in 4H-SiC, reducing their penetration depth into the substrate [10]. Furthermore, the low excess carrier lifetime in the p-emitter necessitates a short distance of the generated electron hole pairs towards the space

charge region. Consequently, a shallow p-emitter is required to shift the space charge region close to the surface. This makes reproducible growth of shallow p+ emitters by epitaxy challenging and ion implantation the method of choice. However, channeling effects of Al in SiC [11] cannot be neglected especially for such shallow emitters. Therefore, different aluminum implantations and their influence on the electrical and optical diode behavior are under investigation in this work. In the following, the way towards the first VUV sensitive 4H-SiC pin-type photodiodes with an implanted emitter is described.

Sample Fabrication

A drawing of the fabricated photodiodes in cross section and top view is shown in Fig. 1. A 6 µm thick epitaxial layer with a nitrogen doping concentration of $9.2 \cdot 10^{14}$ cm^{-3} was grown on a production grade 4H-SiC substrate. In the active region of the diode, a shallow p-emitter was formed by low energy Al ion implantation. In total, four different shallow profiles with single implantation shots using energies ranging from 7.5 keV to 50 keV were investigated as possible p-emitter implantations. Reference diodes only utilized a deeper Al profile with a high doping concentration (EmDeep) as a p-emitter. In addition, the EmDeep profile was implanted at the anode contact for all diodes to ensure proper ohmic contact formation. The respective implantation parameters are listed in Table 1. The dopants were activated at 1700°C for 30 minutes in an Argon atmosphere. Afterwards, a 15 nm thick sacrificial oxide was formed by dry oxidation and subsequently etched with HF. The passivation, which simultaneously works as antireflective coating (ARC), was deposited by two different methods: Low Pressure Chemical Vapor Deposition (LPCVD) using liquid tetraethoxysilane (TEOS) and dry thermal oxidation. Silicidation of TiAl and NiAl were used for p-type and n-type contact formation, respectively.

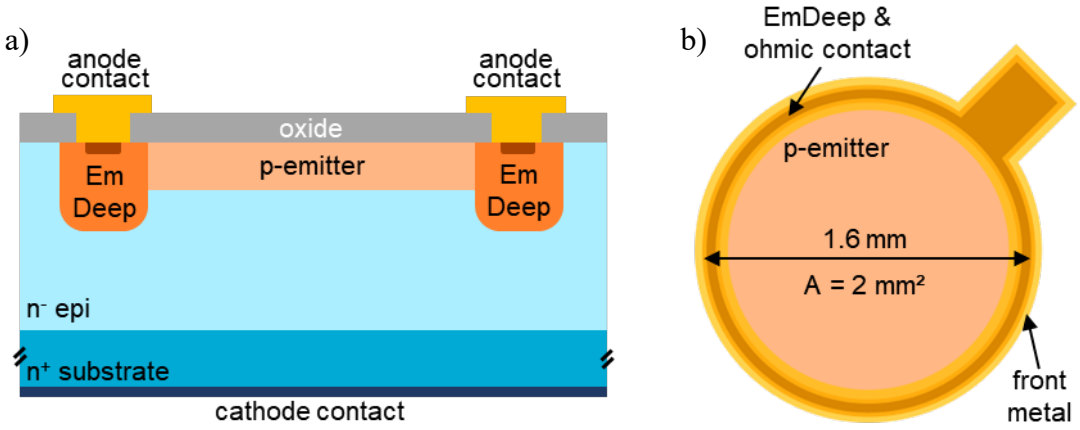

Fig. 1. Diode structure in a) cross section and b) top view.

Table 1. Al implantation parameters for VUV and standard UV diodes

Profile name	Scattering oxide thickness [nm]	Energy [keV]	Dose [cm^{-2}]
7.5 keV	30	7.5	$1.0 \cdot 10^{15}$
20 keV	30	20	$1.0 \cdot 10^{13}$
30 keV	30	30	$1.0 \cdot 10^{13}$
50 keV	30	50	$1.0 \cdot 10^{12}$
EmDeep	30	90	$2.8 \cdot 10^{14}$
		60	$1.8 \cdot 10^{14}$
		30	$1.4 \cdot 10^{14}$

Results and Discussion

The different implantation profiles were analyzed by SIMS measurements directly after the implantation steps, with the results depicted in Fig. 2. Taking the low diffusivity of Al in 4H-SiC with an effective diffusion coefficient of $4.5 \cdot 10^{-16}$ cm² s^{-1} at 1700°C [12] into account, the as-implanted profiles resemble the doping profiles after the annealing steps as a good approximation. In Fig. 2, it can be clearly seen that shallow Al implantations in 4H-SiC using a 30 nm scattering oxide and low implantation energies are possible. In case of the given n-doping of the epitaxial layer, the metallurgical pn-junctions of the diodes with shallow emitter profiles have a depth between 62 nm to 190 nm. Since 46 % of the SiC is consumed during thermal oxidation [3], the pn-junction depth should be reduced by 7 nm for the LPCVD TEOS ARC and 21 nm for the dry oxidation ARC, making it even shallower.

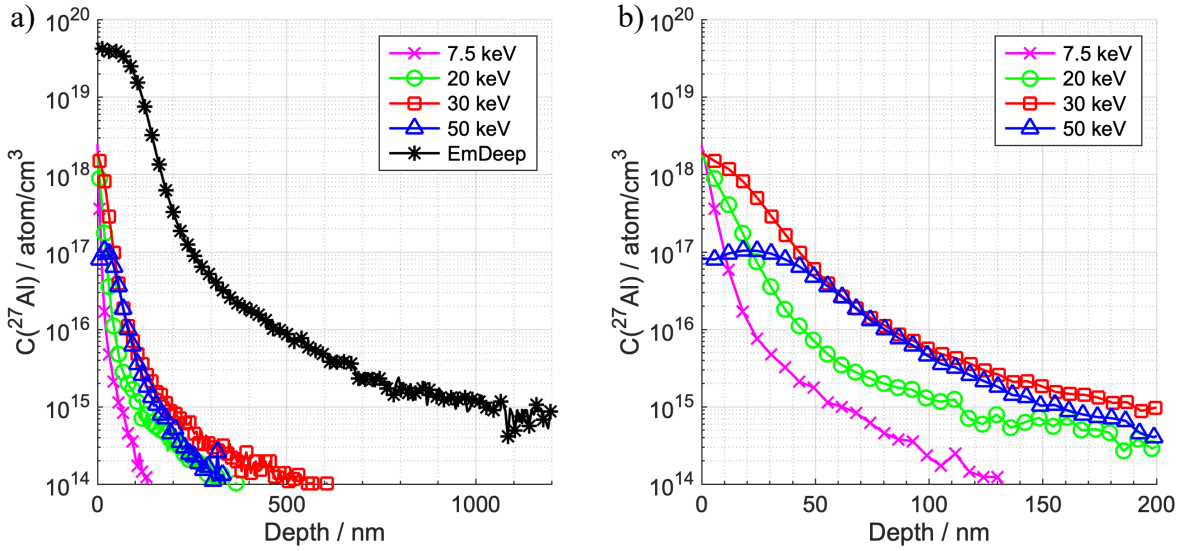

Fig. 2. As-implanted Al-doping profiles determined by SIMS measurement without annealing and origin at SiC surface. Results are shown in a) coarse and b) high resolution of the shallow profiles.

Fig. 3 shows the I-V characteristics of the devices with different doping profiles and for the two different ARC types under illumination with a 280 nm UV-LED. All diode varieties follow typical I-V behavior, although the distinct profiles feature different photocurrents and open circuit voltages. The variance in these values is a result of different sensitivities at the given wavelength. The 7.5 keV dry oxidation ARC profile has a lower parallel resistance since the current is inverse proportional to the voltage between 1 V and -2 V, while the other profiles show a constant current in this voltage range. Thus, these diodes have a high parallel resistance. The comparison of the different ARC types indicates that the usage of a LPCVD TEOS oxide leads to a higher open circuit voltage for all emitter doping profiles. Furthermore, it increases the short circuit current for the shallow emitter profiles. It is assumed that this behavior results from the slightly different doping profiles due to the SiC consumption from the surface during the thermal oxidation step. Another possible explanation could be differences in the SiC/oxide interface, e.g., density of interface states. Hence, the LPCVD TEOS ARC leads to less recombination at the interface and allows a higher sensitivity. In general, the surface Al concentration roughly correlates with the short circuit currents. It is assumed that a lower series resistance is given for a higher surface doping concentration, which causes less charge carrier depletion in the p-doped region at thermodynamic equilibrium. Lower resistance, therefore, allows for a higher short circuit current and sensitivity. Thus, a high Al concentration at the surface is needed to properly collect the generated free carriers during UV absorption at the front side of the diode.

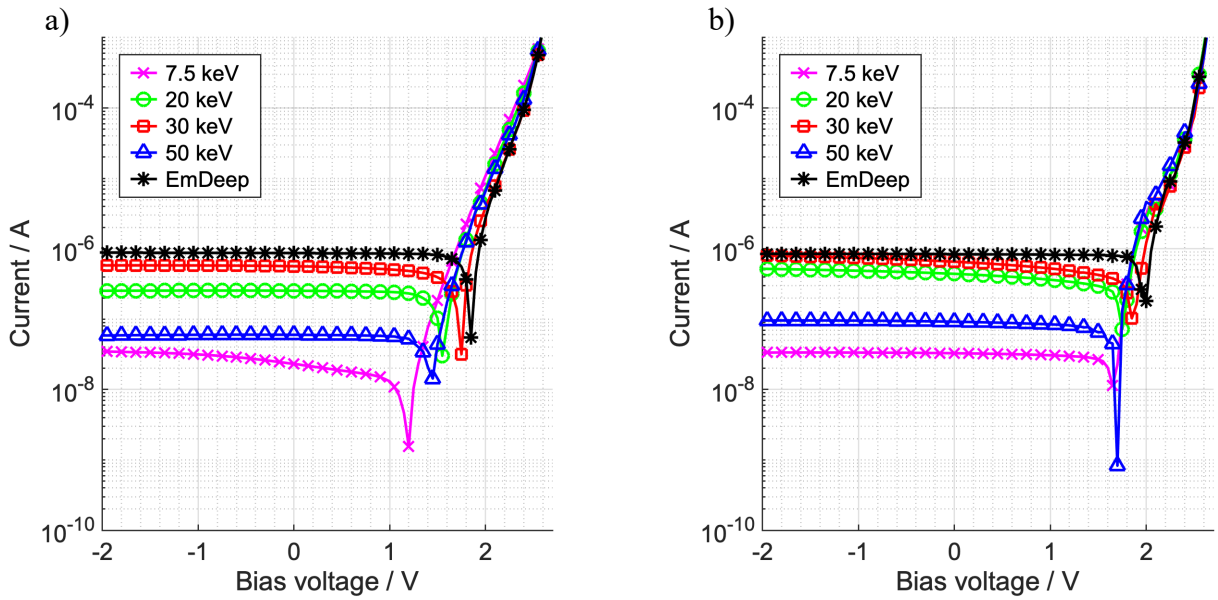

Fig 3. Diode I-V characteristics under illumination of a 280 nm UV-LED with different implantation profiles for a) dry oxidation ARC and b) LPCVD TEOS ARC.

The spectral responsivity (SR) was recorded using a 150 W Xenon light source and a double monochromator DMC150 from Bentham in the wavelength range from 200 nm to 390 nm. A 7.49 mm^2 SiC photodiode calibrated by Physikalisch-Technische Bundesanstalt (PTB), the National Metrology Institute of Germany, served as a reference diode. For the measurements, the incident light beam was split by a polka dot beam splitter and directed into a Si monitoring diode as well as the investigated sample via a concave deflecting mirror. Variations of the incident light intensity are counterbalanced through the measurement of the monitoring diode. SR results, presented in Fig. 4, are displayed as the absolute values, and again normalized to the respective maximum for better visual clarity of the low SR curves. It must be noted that the samples with the profiles 7.5 keV and 20 keV have a LPCVD TEOS ARC whereas the others utilize thermal oxidation ARC. The doping profiles 20 keV, 30 keV and EmDeep show very similar results. This is especially interesting since the metallurgical pn-junctions of the 20 keV and 30 keV profiles are around 120 nm and 190 nm in the as-implanted profile, respectively, while the EmDeep profile has a pn-junction depth of 1 µm. In the SR measurement, the 20 keV and 30 keV profiles have an almost identical responsivity even though the I-V characteristics shows a higher short circuit current for the 30 keV profile. This is attributed to the different used ARC types.

The doping profiles 7.5 keV and 50 keV show weak signals over the whole wavelength range. For the 7.5 keV profile, we assume that the low total amount of donor atoms, which is even more reduced due to the SiC consumption of the oxidation steps, leads to a high sheet resistance and a completely depleted p-emitter. Thus, the current flow is restricted. Additionally, a surface Al concentration of less than $1.0 \cdot 10^{17}$ cm^{-3} in case of the 50 keV profile leads to a high sheet resistance and low overall sensitivity in comparison to the 20 keV, 30 keV and EmDeep profile as well.

Looking at the normalized spectral response, a shift of the peak responsivity towards shorter wavelengths can be observed for the 7.5 keV and 50 keV profiles. Furthermore, a low, but measurable, sensitivity is given for a wavelength of 200 nm. In numbers, the 7.5 keV and 50 keV profiles allow a spectral response of 4.3 mA/W and 8.2 mA/W at 200 nm, respectively, whereas the EmDeep profile has a sensitivity of 0.26 mA/W at the given wavelength. Thus, using the 7.5 keV and 50 keV profiles increases the sensitivity at 200 nm by more than 1500 % and 3000 % compared to the EmDeep profile respectively, while the 20 keV profile leads to a 23 % higher sensitivity and the 30 keV profile shows a 55 % lower signal at 200 nm. Since 200 nm is the upper limit of the VUV range, a sensitivity for the shorter VUV wavelengths can be expected for the 7.5 keV and 50 keV profiles. The 50 keV profile shows slightly higher overall sensitivities even though it uses the

comparatively worse ARC type. For the LPCVD TEOS ARC a higher sensitivity can be anticipated. In conclusion, the generally low doping concentrations of these profiles results in a reasonable sensitivity at a wavelength of 200 nm. However, a significantly lower overall spectral response, probably due to a high series resistance, is observed. Due to the strong absorption of VUV light by oxygen in the atmosphere [1], measurements below wavelengths of 200 nm were not possible for now owing to limitations of the current setup, but are intended in the future. However, the presented results demonstrate the capability of shallow doping profiles for sensing VUV wavelengths using a pin structure. Based on these promising results, further research will be conducted on enhanced diode designs and processing steps to improve the sensitivity not only in the VUV range but also for the longer UV wavelengths.

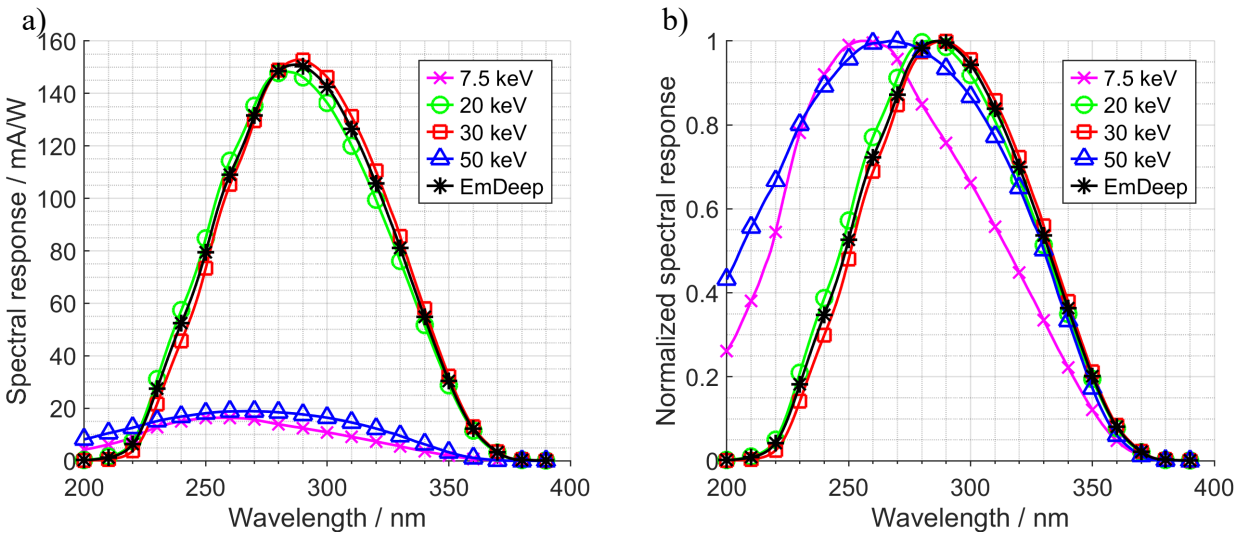

Fig. 4. Spectral response at 0 V bias of diodes with selected emitter profiles. The 7.5 keV and 20 keV profiles used a LPCVD TEOS oxide as an ARC, the others a thermal oxide. Data is displayed as a) absolute values and b) normalized to respective maximum.

Summary

In conclusion, the shallow doping profiles necessary for VUV sensitive pin photodiodes can be realized by ion implantation. Furthermore, some of the investigated shallow emitter doping profiles lead to highly functioning photodiodes comparable to a deep aluminum implantation profile without a VUV sensitivity. The two emitter profiles with the implantation energies 7.5 keV and 50 keV lead to an overall weak spectral response signal, but still allow a noticeable sensitivity at a wavelength of 200 nm. This makes the investigated 4H-SiC photodiodes based on a pin-junction the first ones reported in literature with a sensitivity at this wavelength.

Acknowledgement

This Project is supported by the Federal Ministry for Economic Affairs and Climate Action (BMWK) on the basis of a decision by the German Bundestag.

References

[1] L. Jia, W. Zheng, F. Huang, Vacuum-ultraviolet photodetectors, PhotoniX 1 (2020) 1–25.

[2] Information on https://www.ist-uv.de/de/unternehmen/newsroom/pressemeldungen/pressemeldungen-detail/uv-led-und-excimer-technologie-fuer-holz-und-holzwerkstoffe

[3] T. Kimoto, J.A. Cooper, Fundamentals of Silicon Carbide Technology, John Wiley & Sons Singapore Pte. Ltd, Singapore, 2014.

[4] J. Hu, X. Xin, J.H. Zhao, F. Yan, B. Guan, J. Seely, B. Kjornrattanawanich, Highly sensitive visible-blind extreme ultraviolet Ni/4H-SiC Schottky photodiodes with large detection area, Opt. Lett., OL 31 (2006) 1591–1593.

[5] A. Gottwald, U. Kroth, E. Kalinina, V. Zabrodskii, Optical properties of a Cr/4H-SiC photodetector in the spectral range from ultraviolet to extreme ultraviolet, Applied optics 57 (2018) 8431–8436.

[6] A. Sciuto, M. Mazzillo, S. Di Franco, F. Roccaforte, G. D'Arrigo, Visible Blind 4H-SiC P^{+}-N UV Photodiode Obtained by Al Implantation, IEEE Photonics Journal 7 (2015) 1–6.

[7] C.D. Matthus, T. Erlbacher, A.J. Bauer, L. Frey, Comparative Study of 4H-SiC UV-Sensors with Ion Implanted and Epitaxially Grown p-Emitter, in: 2018 22nd International Conference on Ion Implantation Technology (IIT), IEEE, 2018 - 2018, pp. 110–113.

[8] X. Chen, H. Zhu, J. Cai, Z. Wu, High-performance 4H-SiC-based ultraviolet p-i-n photodetector, Journal of Applied Physics 102 (2007) 24505.

[9] C.D. Matthus, A. Burenkov, T. Erlbacher, Optimization of 4H-SiC Photodiodes as Selective UV Sensors, MSF 897 (2017) 622–625.

[10] A. Burenkov, C.D. Matthus, T. Erlbacher, Optimization of 4H-SiC UV Photodiode Performance Using Numerical Process and Device Simulation, IEEE Sensors J. 16 (2016) 4246–4252.

[11] P. Pichler, T. Sledziewski, V. Häublein, A. Bauer, T. Erlbacher, Channeling in 4H-SiC from an Application Point of View, MSF 963 (2019) 386–389.

[12] M.K. Linnarsson, M.S. Janson, A. Schöner, B.G. Svensson, Aluminum and boron diffusion in 4H-SiC, MRS Online Proceedings Library (OPL) 742 (2002) K6.1.